Astron. Astrophys. 262, 271–280 (1992)

ASTRONOMY AND ASTROPHYSICS

Kinematics of disk planetary nebulae

W.J. Maciel and C.M. Dutra

Instituto Astronômico e Geofísico da USP, Av. Miguel Stefano 4200, CEP 04301 São Paulo SP, Brazil

Received January 2, accepted February 13, 1992

Abstract. The space distribution and kinematic properties of galactic planetary nebulae are considered, on the basis of a sample containing 150 objects. It is shown that planetary nebulae of Types I, IIa, IIb, III, and IV form an approximately continuous sequence in terms of these properties, confirming similar conclusions based on their chemical composition. Some kinematical consequences regarding the connection between planetary nebulae and H II regions are explored, leading to a determination of the galactic rotation curve and Oort's constants. It is found that the rotation curve presents a flattening near the solar circle and a moderate increase for larger galactocentric distances.

Key words: planetary nebulae – kinematics – rotation curve

1. Introduction

It has become clear that planetary nebulae (PN) constitute a true stage in stellar evolution, especially regarding their chemical composition (cf. Peimbert 1990; Maciel 1992). In fact, as the offspring of stars having a considerable mass range at the main sequence, PN are expected to present a certain amount of variety not only in their chemical composition but also regarding their space distribution and kinematics.

Based on these properties, an attractive classification scheme has been proposed by Peimbert (1978), which has been later extended and refined (Peimbert & Torres-Peimbert 1983; Faúndez-Abans & Maciel 1987; Maciel 1989). According to this scheme, Type I PN are ejected from the most massive of the intermediate mass stars, and present strong He and N enrichment. Type II form the bulk of disk PN, being further subdivided into IIa (some N enrichment, intermediate between Type I and Type IIb) and IIb (no N enrichment). Type III are nebulae ejected from older stars, reaching higher distances from the galactic plane and presenting definite underabundances of heavy elements. Finally, Type IV include the few known PN in the galactic halo, and Type V are the nebulae found in the galactic centre.

In the past few years, we have applied such classification scheme to a sample of galactic planetary nebulae for which a detailed amount of data exists (Maciel & Faúndez-Abans 1985; Faundez-Abans & Maciel 1986, 1987; Maciel 1987, 1992). Such data include basically electron temperatures (mainly from the [O III] lines) and densities, chemical composition (He, C, N, O, S, Ne, Ar, and Cl), distances and radial velocities. In the previous papers, we have considered in greater detail the chemical composition of the nebulae, especially regarding their classification and the existence of galactic gradients. On the other hand, the kinematical properties of PN make them interesting objects to study the kinematics of the disk population, as has been shown by Schneider & Terzian (1983) and Peralta (1978). In particular, there are controversies regarding the rotation curve of the Galaxy outside the solar circle, and it is not clear whether the curve decreases, remains constant or even increases thereafter (see, for example, Blitz 1979; Blitz et al. 1980; Burton & Gordon 1978; Knapp 1983; Chini & Wink 1984; Clemens 1985; Rohlfs et al. 1986). Since PN are luminous objects that can be observed to relatively large distances and have accurately measured velocities, it is interesting to investigate their possible contribution to this problem.

In the present work, we will explore the kinematical properties of the different types of PN in comparison with classical population I objects. We will concentrate on the space distribution and kinematics of disk nebulae, especially considering the determination of the galactic rotation curve and of Oort's constants. Some preliminary results of this work have been presented earlier by Dutra & Maciel (1990).

2. The data

The data sample is an evolved and updated form of the list of objects studied by Maciel & Faúndez-Abans (1985) and Faúndez-Abans & Maciel (1986, see also Maciel 1992). The reader is referred to these papers for further details on the classification criteria. Tables 1–5 present the basic data for PN of Types I, IIa, IIb, III, and IV, respectively. The tables give (1) the common name, (2) the PK number, (3) the galactic longitude, (4) the galactic latitude, (5) the adopted distances (kpc) with (6) the original sources and (7) the measured radial velocities relative to the Local Standard of Rest, V_{LSR}.

Most of the distances come from the catalogue by Maciel (1984), derived on the basis of a mass-radius relationship. For several objects, however, more accurate values have been adopted, according to the reference list supplementing the tables. These are generally distances obtained by individual astrophysical methods, so that the adopted values are as accurate as possible in a statistical study. On the other hand, the main results of this paper are essentially unaffected if we adopt a different set of

Send offprint requests to: W.J. Maciel

Table 1. Data for Type I planetary nebulae

Name	PK	l	b	d (kpc)	Ref.	V_{LSR} (km s^{-1})
NGC 650	130−10 1	130.94	−10.51	0.7	1	−16.1
NGC 2346	215+03 1	215.70	3.61	1.5	1	5.4
NGC 2440	234+02 1	234.84	2.43	1.1	1	44.9
NGC 2452	243−01 1	243.39	−1.04	2.7	1	50.0
NGC 2818	261+08 1	261.98	8.60	2.3	1	−16.8
NGC 3132	272+12 1	272.12	12.39	1.1	1	−28.5
NGC 5189	307−03 1	307.22	−3.47	0.7	1	−15.1
NGC 5315	309−04 2	309.18	−4.43	0.7	2	−39.3
NGC 6153	341+05 1	341.84	5.46	1.0	1	44.9
NGC 6302	349+01 1	349.51	1.05	0.4	1	−31.4
NGC 6369	002+05 1	2.44	5.85	0.6	1	−90.0
NGC 6445	008+03 1	8.07	3.90	1.0	1	29.0
NGC 6537	010+00 1	10.10	0.73	0.7	2	−4.1
NGC 6620	005−06 1	5.88	−6.15	4.0	1	83.6
NGC 6629	009−05 1	9.41	−5.06	1.6	1	26.6
NGC 6741	033−02 1	33.81	−2.68	1.7	1	57.9
NGC 6751	029−05 1	29.22	−5.93	2.8	1	−23.0
NGC 6778	034−06 1	34.61	−6.71	2.2	1	107.0
NGC 6781	041−02 1	41.84	−2.98	0.9	1	21.5
NGC 6803	046−04 1	46.44	−4.13	2.5	1	30.4
NGC 6804	045−04 1	45.75	−4.59	1.6	1	5.3
NGC 6853	060−03 1	60.83	−3.69	0.4	1	−24.3
NGC 6881	074+02 1	74.55	2.12	1.7	1	2.9
NGC 7008	093+05 2	93.42	5.49	0.9	1	−60.9
NGC 7293	036−57 1	36.17	−57.16	0.2	1	−25.0
NGC 7354	107+02 1	107.84	2.31	0.8	1	−30.6
IC 4406	319+15 1	319.69	15.74	1.7	1	−40.2
IC 4673	003−02 3	3.56	−2.44	3.4	1	−4.9
H1-18	357+02 1	357.63	2.60	2.9	5	−193.9
H1-23	357+01 1	357.61	1.80	3.3	3	−62.0
H2-18	006+04 1	6.38	4.46	3.9	1	−103.5
Hb 4	003+02 1	3.17	2.93	2.2	1	−51.1
Hb 5	359−00 1	359.35	−0.98	1.2	1	−17.9
Hb 6	007+01 1	7.28	1.85	1.9	1	21.7
He2-111	315−00 1	315.02	−0.38	2.8	1	−12.5
Hu1-2	086−08 1	86.54	−8.83	2.2	1	24.0
K3-61	096+02 1	96.31	2.34	1.1	1	
M1-8	210+01 1	210.32	1.92	3.5	1	35.8
M1-13	232−01 1	232.40	−1.85	4.4	1	27.7
M1-17	228+05 1	228.84	5.36	5.8	1	82.8
M1-35	003−02 1	3.92	−2.32	2.7	3	93.1
M1-41	006−02 1	6.76	−2.24	1.4	1	7.1
M1-42	002−04 2	2.73	−4.85	4.0	1, 2, 3	−83.8
M1-75	068−00 1	68.86	−0.05	2.8	3	8.5
M2-55	116+08 1	116.30	8.54	1.9	1	−12.9
Me1-1	052−02 2	52.54	−2.96	3.8	1	11.7
Me2-2	100−08 1	100.03	−8.75	2.8	4	−140.5
Mz 3	331−01 1	331.74	−1.03	1.0	1	−19.2
PB 4	275−04 1	275.06	−4.18	2.9	1	
PB 6	278+05 1	278.85	5.00	4.0	1	
Vy1-1	118−08 1	118.06	−8.68	1.9	3	−43.4
Vy2-2	045−02 1	45.50	−2.71	1.9	1	−53.9
Ym 29	205+14 1	205.14	14.25	0.3	2	15.4

References (see Table 5)

Table 2. Data for Type IIa planetary nebulae

Name	PK	l	b	d (kpc)	Ref.	V_{LSR} (km s^{-1})
NGC 2371	189+19 1	189.16	19.83	1.5	1	11.4
NGC 2392	197+17 1	197.88	17.40	2.0	6	63.4
NGC 2438	231+04 2	231.81	4.14	1.5	1	58.7
NGC 2867	278−05 1	278.17	−5.93	1.6	1	0.4
NGC 3587	148+57 1	148.50	57.06	0.7	1	11.5
NGC 3918	294+04 1	294.69	4.71	2.2	7	−24.5
NGC 5882	327+10 1	327.84	10.09	1.6	1	11.9
NGC 6309	009+14 1	9.66	14.81	2.1	1	−33.4
NGC 6565	003−04 5	3.54	−4.61	1.5	8	6.2
NGC 6572	034+11 1	34.62	11.82	0.8	1	9.6
NGC 6578	010−01 1	10.82	−1.83	2.1	1	17.3
NGC 6720	063+13 1	63.15	13.98	0.7	1	0.0
NGC 6818	025−17 1	25.86	−17.90	1.5	1	−1.3
NGC 6886	060−07 2	60.14	−7.74	1.7	9	−18.9
NGC 6894	069−02 1	69.48	−2.62	1.5	1	−40.8
NGC 6905	061−09 1	61.50	−9.58	1.8	1	8.1
NGC 7009	037−34 1	37.76	−34.58	0.9	1	−36.5
NGC 7026	089+00 1	89.00	0.37	0.9	1	−25.6
NGC 7027	084−03 1	84.92	−3.49	0.7	1	24.0
IC 1747	130+01 1	130.26	1.40	2.5	9	−61.8
IC 2003	161−14 1	161.03	−14.90	2.4	1	−22.3
IC 2149	166+10 1	166.14	10.47	1.1	2	−35.8
IC 2165	221−12 1	221.33	−12.40	1.9	1	35.2
IC 2448	285−14 1	285.79	−14.95	2.9	1	−36.9
IC 2501	281−05 1	281.00	−5.69	0.8	2	19.5
IC 5117	089−05 1	89.87	−5.14	1.0	2	−12.0
IC 5217	100−05 1	100.62	−5.40	2.8	1	−86.7
Cn2-1	356−04 1	356.29	−4.41	3.6	1	−262.2
Hu1-1	119−06 1	119.67	−6.77	4.7	3	−46.9
M1-74	052−04 1	52.22	−4.01	2.5	4	27.5
M1-80	107−02 1	107.78	−2.29	6.4	2	−47.4
M3-15	006+04 2	6.80	4.17	1.9	5	112.8

References (see Table 5)

distances from a unique source, such as Acker (1978) or Daub (1982).

The radial velocities are from the catalogue by Schneider et al. (1983), with estimated errors lower or about 10 km s^{-1}. For a few objects the errors may be larger, especially if only one old measurement (e.g. 1918) is available, as mentioned in the next section.

3. Space distribution and kinematics

Given the galactic coordinates (l, b) and the distance of a nebula, its height Z from the galactic plane and the galactocentric distance R projected on the plane can be calculated for an assumed distance R_0 between the Sun and the galactic centre. The value of R_0 has been generally placed in the range 7–11 kpc (see for example Knapp 1983), and recent work points to values closer to 8 kpc (Reid 1989). In order to make comparisons with recently published rotation curves, we have adopted in this papar $R_0 = 8.5$ kpc. However, the main conclusions are essentially unchanged if the old IAU value $R_0 = 10$ kpc is used. For disk objects, we assume pure circular rotation, adopting three different rotation curves: (i) the "short" curve by Clemens (1985), with $R_0 = 8.5$ kpc and rotation velocity at the Sun's position $\Theta_0 = 220$ km s^{-1}; (ii) the "long" curve by Clemens (1985), with $R_0 = 10$ kpc and $\Theta_0 = 250$ km s^{-1} and (iii) the curve given by Burton & Gordon (1978) for $R < R_0$ and by Blitz et al. (1980) for $R > R_0 = 10$ kpc.

The peculiar radial velocity ΔV can be defined as

$$\Delta V = V_{LSR} - R_0\left[\frac{\Theta(R)}{R} - \frac{\Theta_0}{R_0}\right]\sin l \cos b, \quad (1)$$

where $\Theta(R)$ is the rotation velocity at the nebula galactocentric position calculated for a given rotation curve. Similarly, we can also define the direct deviation from the adopted rotation curve (cf. Maciel 1987; Dutra & Maciel 1990) by

$$\Delta\Theta = \left[\frac{V_{LSR}}{\sin l \cos b} + \Theta_0\right]\frac{R}{R_0} - \Theta(R). \quad (2)$$

Figure 1 shows the distribution of PN of Types I, II and III, respectively, according to the height from the galactic plane. For

Table 3. Data for Type IIb planetary nebulae

Name	PK	l	b	d (kpc)	Ref.	V_{LSR} (km s^{-1})
NGC 40	120+09 1	120.02	9.87	0.8	1	−11.6
NGC 1535	206−40 1	206.48	−40.57	1.6	1	−20.0
NGC 2022	196−10 1	196.68	−10.93	2.2	1	−1.3
NGC 2792	265+04 1	265.77	4.10	1.8	1	−1.0
NGC 3211	286−04 1	286.31	−4.88	2.5	1	−34.4
NGC 3242	261+32 1	261.06	32.06	0.8	1	−5.3
NGC 5307	312+10 1	312.38	10.56	2.3	1	37.3
NGC 6210	043+37 1	43.12	37.76	1.3	1	−17.7
NGC 6543	096+29 1	96.47	29.95	0.7	1	−50.7
NGC 6567	011−00 2	11.75	−0.65	1.5	2, 10	132.9
NGC 6790	037−06 1	37.93	−6.37	1.5	1	56.8
NGC 6826	083+12 1	83.57	12.49	0.7	1	10.9
NGC 6879	057−08 1	57.23	−8.93	3.7	1	25.7
NGC 6884	082+07 1	82.14	7.10	1.7	1	−18.7
NGC 6891	054−12 1	54.20	−12.11	2.2	1	58.6
NGC 7662	106−17 1	106.56	−17.60	0.8	1	−4.7
IC 351	159−15 1	159.05	−15.19	3.0	1	−15.3
IC 418	215−24 1	215.22	−24.27	1.6	6	43.4
IC 3568	123+34 1	123.66	34.55	2.1	1	−31.6
IC 4776	002−13 1	2.10	−13.45	3.3	1	27.9
BD+303639	065+05 1	64.78	5.02	0.7	2	−13.0
Hb 12	111−02 1	111.88	−2.86	2.3	3	4.5
J 320	190−17 1	190.39	−17.77	4.1	1	−37.9
J 900	194+02 1	194.24	2.59	2.1	1	33.8
M1-1	130−11 1	130.36	−11.74	4.1	3, 2	−35.1
M1-4	147−02 1	147.40	−2.31	1.7	2	−34.1
M1-5	184−02 1	184.05	−2.14	2.1	1	25.7
M2-2	147+04 1	147.87	4.19	1.4	1	−7.4

References (see Table 5)

comparison, the distribution of kinematically distinct CO–H II region complexes from Blitz et al. (1982) is also shown in the first panel of Fig. 1. We selected the objects in the same range of galactocentric distances as the PN sample, that is, $4 < R(\text{kpc}) < 14$, which is approximately equivalent to an upper distance limit $d = 4$ kpc. The increase in the average height from Type I to III can be clearly seen. Within Type II PN, some increase is also obtained, in the sense that Type IIa are in average closer to the galactic plane than Type IIb objects. These results are better seen in Table 6, where we give the number n of objects, the average height $\langle|Z|\rangle$ of the sample, the standard deviation σ and the median $|Z_{1/2}|$. Although the *absolute* value of the averages may be affected by the incompleteness of the sample, the similarity between $\langle|Z|\rangle$ and $|Z_{1/2}|$ and especially the *relative* average heights clearly indicate a progressive increase of the distance to the galactic plane for PN of Types I, IIa, IIb, III and IV. Of course, for the latter the averages should be viewed with caution, as there are only 6 nebulae in this class.

Regarding the bulk of disk PN, which are mainly Type II objects, the average height from Table 6 is 240–350 pc, probably closer to the first value. This is consistent with Population I Disk characteristics (cf. Maciel & Leite 1992), and is in good agreement with the recent determination of the PN scale height by Zijlstra & Pottasch (1991).

Figure 2 shows histograms of the peculiar velocity ΔV from Eq. (1) for H II regions and PN of Types I, II and III. Here we have used the Clemens (1985) curve for $R_0 = 8.5$ kpc, but it should be stressed that the results are unchanged for the other two curves. It is seen that the average peculiar velocity also increases from Type I to III, although the absolute values for Types I and II are similar. Some distinction can also be made between Type IIa and IIb, as shown in Table 6, where the averages $\langle|\Delta V|\rangle$ and $|\Delta V_{1/2}|$ are defined analogously to the scale height averages. Again, the curve by Clemens (1985) with $R_0 = 8.5$ kpc was used.

The PN sample used in the estimate of the average peculiar velocity is smaller, as we must exclude those objects with high velocities near the direction of the galactic centre, where the uncertainties are higher, since the velocities vary rapidly (see for example Maciel 1989, Fig. 2), and non-circular motions occur. Also, some nebulae have no measured radial velocities, and a few others have only one measurement, generally old and made at low dispersion, so that their uncertainty is also higher than for most objects.

Histograms for the deviation $\Delta\Theta$ calculated from (2) can also be obtained, with similar results to those presented for ΔV in Fig. 2 and Table 6, except that the deviation is more sensitive to the position of the nebula, due to the factor $\sin l \cos b$ in Eq. (2).

As a conclusion, from Figs. 1 and 2 and Table 6 an approximately continuous sequence of objects can be observed, in the following order: H II regions, PN of Types I, IIa, IIb, III, and IV. This is better seen in Fig. 3, where the average values for Z, ΔV and $\Delta\Theta$ are plotted both for the sample averages (circles, upper

Table 4. Data for Type III planetary nebulae

Name	PK	l	b	d (kpc)	Ref.	V_{LSR} (km s^{-1})
NGC 246	118−74 1	118.82	−74.71	0.4	1	−51.0
NGC 1360	220−53 1	220.33	−53.91	0.3	1	25.6
NGC 1514	165−15 1	165.53	−15.29	0.8	1	51.7
NGC 2242	170+15 1	170.31	15.87	4.0	11	15.0
NGC 2610	239+13 1	239.54	13.95	2.6	1	72.3
NGC 4361	294+43 1	294.11	43.62	0.9	1	7.9
NGC 6439	011+05 1	11.00	5.90	3.8	1	−80.1
NGC 6644	008−07 2	8.39	−7.32	2.8	3	205.3
NGC 6807	042−06 1	42.96	−6.93	5.5	1	−51.0
NGC 6833	082+11 1	82.53	11.36	1.2	2	−91.6
IC 4593	025+40 1	25.41	40.73	2.4	1	38.7
IC 4634	000+12 1	0.38	12.22	2.5	1	−21.3
IC 4732	010−06 1	10.80	−6.49	3.4	1	−133.3
IC 4846	027−09 1	27.61	−9.46	2.8	3	165.7
IC 4997	058−10 1	58.34	−10.98	1.2	2	−49.8
A 50	078+18 1	78.53	18.72	2.8	1	−141.0
Cn3-1	038+12 1	38.26	12.09	2.9	1	22.5
Hb-8	003−17 1	3.90	−17.12	5.3	1	−163.4
He2-108	316+08 1	316.17	8.45	3.9	1	−9.6
He2-131	315−13 1	315.11	−13.08	1.6	1	−5.9
Hu2-1	051+09 1	51.48	9.69	1.2	2	33.0
K3-67	165−06 1	165.54	−6.57	3.5	2	−84.2
M1-26	358−00 2	358.95	−0.73	1.6	6	5.0
M1-78	093+01 1	93.54	1.48	3.1	1	−73.8
M2-6	353+06 2	353.35	6.32	4.1	5	−79.3
M2-9	010+18 2	10.91	18.06	3.3	1	102.7
M2-23	002−02 4	2.22	−2.78	2.6	5	234.7
M2-50	097−02 1	97.68	−2.46	4.8	3	−123.1
M4-3	357+07 1	357.23	7.41	3.2	5	166.5
Me2-1	342+27 1	342.14	27.53	4.0	1	53.6
Sn 1	013+32 1	13.30	32.73	5.4	4	−71.7
SwSt-1	001−06 2	1.58	−6.71	1.2	12	−8.7
Vy1-2	053+24 1	53.35	24.06	4.7	1	−82.4

References (see Table 5)

Table 5. Data for Type IV planetary nebulae

Name	PK	l	b	d (kpc)	Ref.	V_{LSR} (km s^{-1})
BB-1	108−76 1	108.42	−76.18	13.5	4, 11	191.5
DDM-1	061+41 1	61.94	41.40	12.0	13	−285.6
Ha4-1	049+88 1	49.05	88.15	7.8	1, 4, 11	−133.1
K648	065−27 1	65.02	−27.32	13.0	1, 3, 4	−128.1
PRMG-1	006−41 1	6.17	−41.96	7.7	14	
PRTM-1	242−37 1	242.17	−37.11	5.0	15	

References for Tables 1–5: (1) Maciel (1984), (2) Daub (1982), (3) Acker (1978), (4) Acker (1980), (5) Amnuel et al. (1984), (6) Méndez et al. (1992), (7) Gathier et al. (1986a), (8) Maciel et al. (1986), (9) Gathier et al. (1986b), (10) Sabbadin (1986), (11) Torres-Peimbert et al. (1990), (12) Freitas Pacheco & Veliz (1987), (13) Barker & Cudworth (1984), (14) Peña et al. (1989), (15) Peña et al. (1990).

curve in each panel), and medians (squares, lower curves). In Fig. 3, object 1 stands for H II regions, object 2 = Type I PN, object 3 = Type IIa, object 4 = Type IIb, object 5 = Type III, and object 6 = Type IV. It is interesting that the average values shown in Fig. 3 (circles) are generally higher than the medians (squares), meaning that the probability distributions extend farther for larger heights and velocities than for shorter values of these quantities. This probably reflects the formation history of the

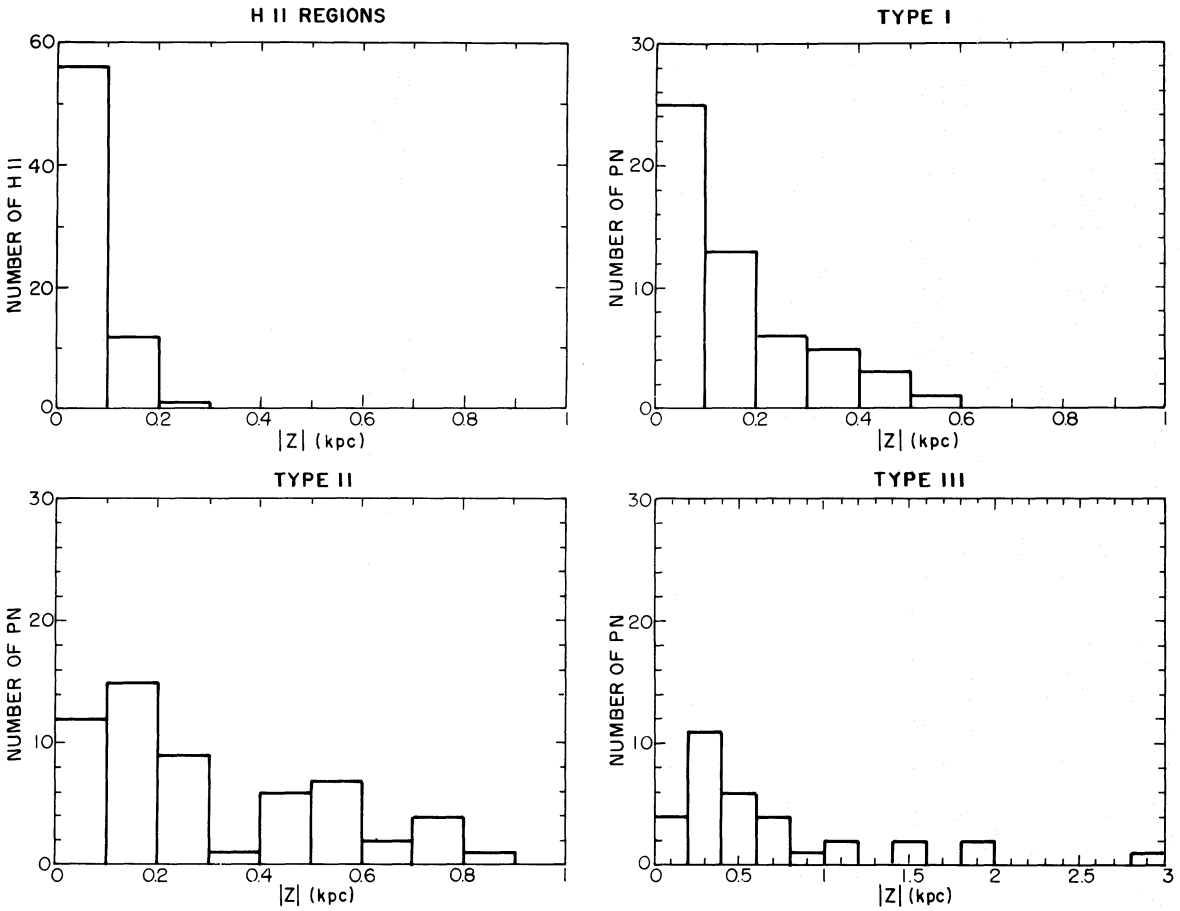

Fig. 1. Distribution of the heights from the galactic plane for H II regions (upper left panel), Type I PN (upper right), Type II PN (lower left), and Type III (lower right)

Table 6. Average distances from the galactic plane and peculiar velocities

Type	n	$\langle\|Z\|\rangle$ (pc)	σ (pc)	$\|Z_{1/2}\|$ (pc)	n	$\langle\|\Delta V\|\rangle$ (km s^{-1})	σ (km s^{-1})	$\|\Delta V_{1/2}\|$ (km s^{-1})
H II	69	60	50	40	69	6.6	5.9	4.5
I	53	150	130	110	38	20.5	14.1	17.2
IIa	32	280	210	220	30	21.3	17.3	18.0
II	60	350	300	240	57	21.7	16.5	20.9
IIb	28	420	360	300	27	22.1	16.0	21.0
III	33	660	640	410	29	64.0	45.0	57.1
IV	6	7200	3400	6900	4	172.8	82.9	167.2
I+IIa	85	200	180	140	68	20.9	15.5	17.2
I+II	113	260	250	170	95	21.2	15.6	19.3

sample, producing a continuous sequence of objects, from the oldest (Type IV PN, or, more exactly, their central stars) to the youngest (H II regions). As a consequence, the variation within the PN class is also approximately continuous, so that the different types should be viewed as representative types of different populations.

4. PN and the galactic rotation curve

The determination of the galactic rotation curve is normally based on the positions and kinematics of young population I objects, such as H II regions or H II/CO complexes. However, other classes of objects belonging to later populations may also

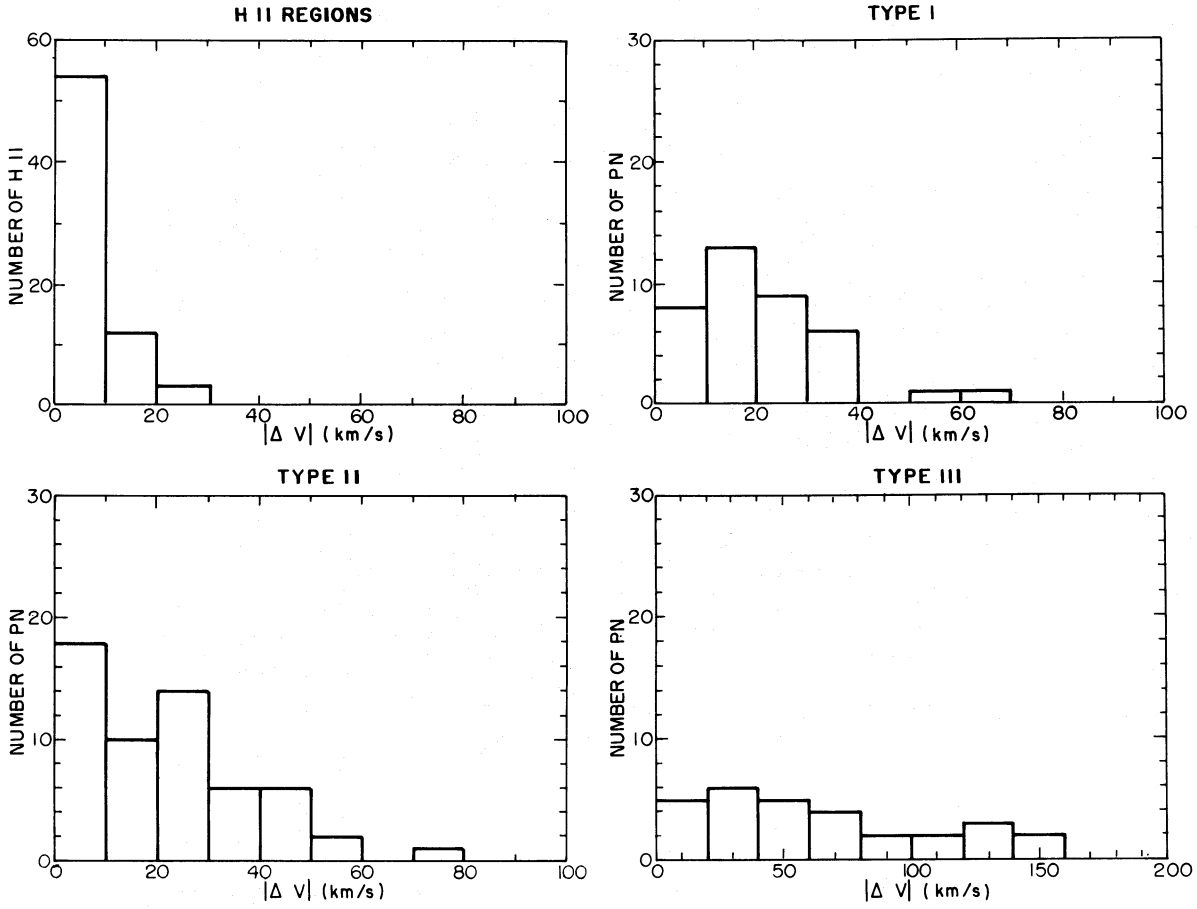

Fig. 2. Distribution of the peculiar velocity [cf. Eq. (1)] for H II regions (upper left panel), Type I PN (upper right), Type II PN (lower left), and Type III (lower right)

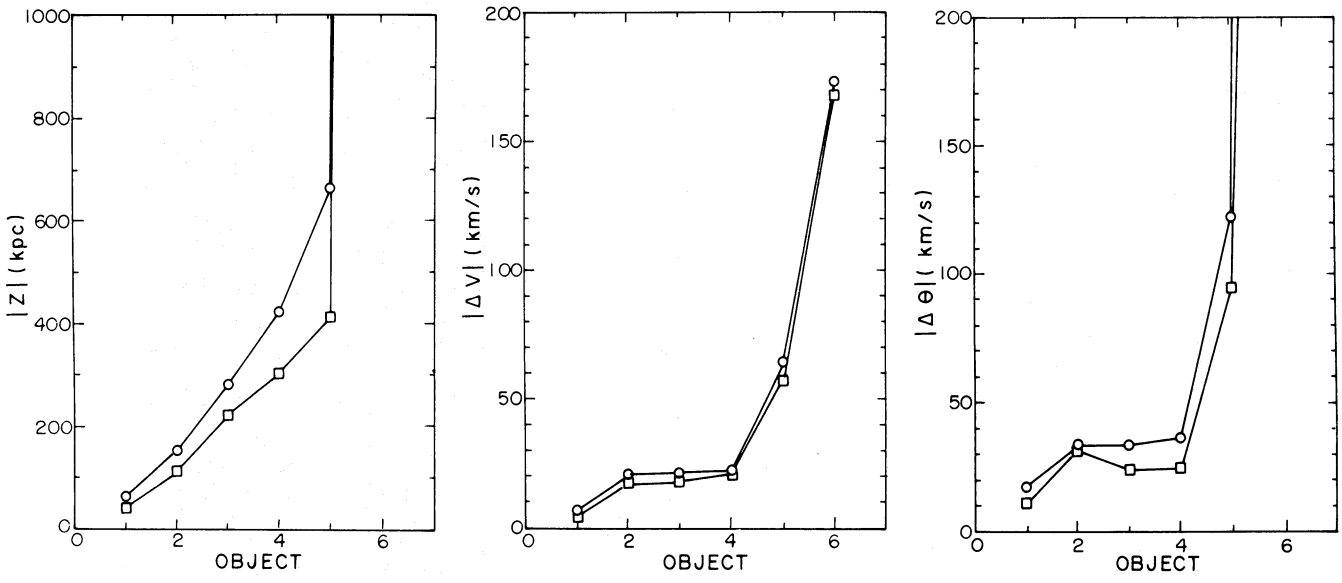

Fig. 3. Comparison of average heights to the galactic plane (left panel), peculiar velocities (middle panel), and deviation from an average rotation curve (right panel) for several kinds of objects: object 1: H II regions; object 2: Type I PN; object 3: Type IIa PN; object 4: Type IIb PN; object 5: Type III PN; object 6: Type IV PN. The higher curves in each panel (circles) are the *mean* values, and the lower curves (squares) are the *medians*

give some contribution to this problem, especially when they are bright, numerous and with reasonably accurate positions and velocities. As discussed by Schneider & Terzian (1983) and Maciel (1987, 1989), PN fulfil these conditions, provided we have some means of selecting the younger PN populations.

Given the results of Sect. 3, it is interesting to investigate the possibility of using the present sample of disk planetary nebulae to establish the galactic rotation curve. In Fig. 4 we plot part of the Clemens (1985) curve for $R_0 = 8.5$ kpc, along with the H II regions and PN of Types I, IIa, and IIb. Here again we are excluding objects near the direction of the galactic centre. It can be seen that the dispersion of the data relative to the curve generally increases from the upper left panel to the lower right panel. In particular, the higher dispersion of Type IIb relative to Type IIa is clearly seen. For Type III (not shown in Fig. 4) the dispersion is very high, and essentially no association is obtained with the rotation curve, as expected.

The same behaviour displayed in Fig. 4 can be observed if the long ($R_0 = 10$ kpc) Clemens (1985) curve or the curves by Burton & Gordon (1978) and Blitz et al. (1980) are used. In fact, the main discrepancy between those curves occurs for $10 < R(\text{kpc}) < 14$, where the curve by Clemens has systematically lower velocities, the difference averaging 10 km s^{-1}, which is smaller than the dispersion presented by our data.

On the basis of the results shown in Table 6 and Figs. 1–4, we have fitted second- and third-order polynomials to the data points, which are shown in Fig. 5 along with the corresponding data for PN of Types I, I + IIa, and I + II, for which the results are more significant, in view of the larger size of the samples. The H II region data and corresponding polynomials are also shown for comparison. In all cases plotted, both polynomials produce essentially the same results in the range $6 < R(\text{kpc}) < 12$, where most objects are concentrated. The curves can therefore be approximated by a second-order polynomial

$$\Theta(R) = a + bR + cR^2 \qquad (3)$$

where the coefficients a, b, c are given in Table 7. An estimate of the goodness of the fit can be given by the rms velocity deviation, which is 35–40 km s^{-1} for the PN sample, depending on the consideration or not of objects near the galactic centre and anticentre. For H II regions we obtain deviations of 16–25 km s^{-1}, which is consistent with the value of 17 km s^{-1} derived by Rohlfs et al. (1986) on the basis of a much larger and selected sample of H II regions in a recent determination of the rotation curve. Therefore, the dispersion is about 10–20 km s^{-1} higher for PN than for H II regions, as could be expected from Table 6. However, the general behaviour of the curves are similar, so that planetary nebulae of types I + IIa (or I + II) can be used to obtain a good estimate of the rotation curve, especially at higher galactocentric radii, provided a larger sample is considered. As mentioned in Sect. 1, it is not clear whether the curve falls down for $R > R_0$, as expected in a pure keplerian orbit, or stays constant

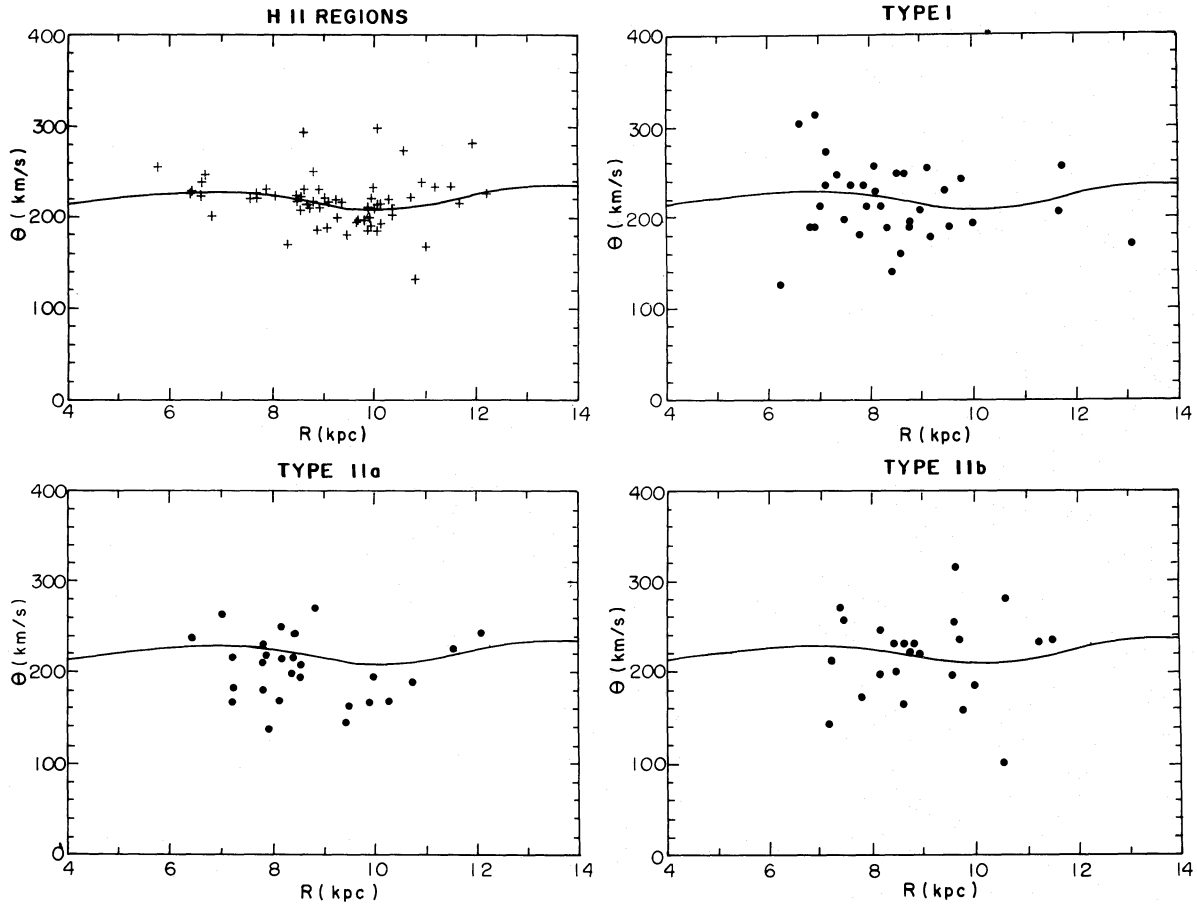

Fig. 4. Rotation velocities as a function of the galactocentric distance for H II regions (upper left panel), Type I PN (upper right), Type IIa PN (lower left) and Type IIb (lower right). The continuous line is the rotation curve by Clemens (1985) for $R_0 = 8.5$ kpc and $\Theta_0 = 220$ km s^{-1}

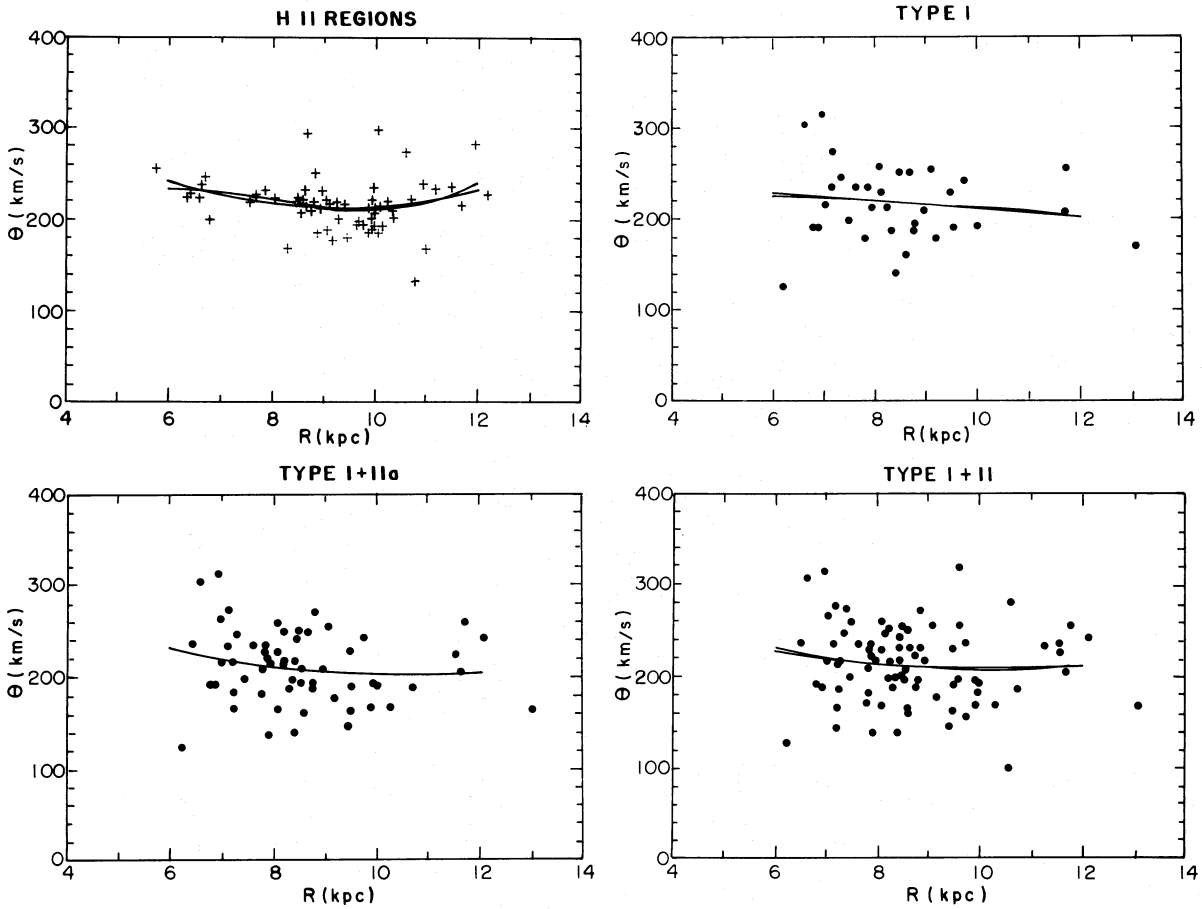

Fig. 5. Rotation velocities as a function of the galactocentric distance for H II regions (upper left panel), Type I PN (upper right), Types I+IIa PN (lower left), and Types I+II PN (lower right). The continuous lines are second- and third- order polynomials fitted to the data

Table 7. Polynomial coefficients and Oort's constants

Name	*a*	*b*	*c*	*A*	*B*
H II	445.0267	−50.1568	2.6968	14.72	−10.41
Type I	230.9705	0.4873	−0.2567	14.68	−10.80
Type I+IIa	365.6274	−30.9711	1.4618	15.29	−9.17
Type I+II	314.1356	−20.5234	0.9855	14.29	−10.52

or even increases (Blitz et al. 1980). Our best curve suggests a flattening up to $R \approx 10.5$ kpc followed by a moderate increase at larger radii. However, few nebulae in our sample have $R > 12$ kpc, so that more data would be needed to further investigate this question.

Planetary nebulae have also been used by Schneider & Terzian (1983) in order to determine the galactic rotation curve, stressing on the problem of the PN distance scale. Our approach differs from theirs in that we emphasize the characteristics of the PN sample derived from their space distribution and chemical composition apart from the kinematic properties, so that we can divide the analysis according to the PN types. Despite of that, our curves given by the polynomial fit (3) do not differ very much from the curve obtained by Schneider & Terzian (1983) in the range $6 < R(\text{kpc}) < 12$, which is partly due to the fact that the radial velocities are from the same source (Schneider et al. 1983). As discussed above, we cannot confirm the *sharp* increase of the rotation curve as proposed by Schneider & Terzian (1983) and Blitz (1983). However, the results presented in Fig. 5 and Table 6 suggest a moderate increase and clearly seem to exclude any further *decrease* of the curve in that region. In fact, our curves are similar to the curve by Rohlfs et al. (1986) for H II regions, provided their curve is scaled to $R_0 = 8.5$ kpc and $\Theta_0 = 220\ \text{km s}^{-1}$.

As in the analysis by Schneider & Terzian (1983), planetary nebulae present slightly lower velocities near R_0 as compared to H II regions. This is probably due to the asymmetric drift, which was not compensated for in this work. Schneider & Terzian (1983)

estimate an average drift of 15 km s^{-1} for their sample. From Table 6 we estimate this to be somewhat lower, around 10 km s^{-1} for PN of Types I and II.

In the present analysis, it has been assumed that disk objects have pure circular motions around the galactic centre. However, non-circular motions are known to exist in the Galaxy, so that the dispersions of Table 6 and Fig. 5 may be partially due to them. For the planetary nebulae of our sample their influence is probably small, as (i) PN are evolved objects not particularly sensitive to local asymmetries, and (ii) radial flows are more important for the objects near the direction of the centre (see for example Knapp 1983), which were excluded from the kinematical analysis up to 5 kpc from the centre. Also, part of the dispersion can be attributed to peculiar motions associated with the LSR itself, which amount to 5 km s^{-1} in the radial direction and 7 km s^{-1} in the azimuthal direction (Clemens 1985; Shuter 1982).

As a check on the consistency of the rotation curves obtained, one can use the curves shown in Fig. 5 in order to determine Oort's constants A and B. This could be done simply by applying the definitions

$$A=\frac{1}{2}\left[\frac{\Theta_0}{R_0}-\left(\frac{d\Theta}{dR}\right)_0\right], \quad (4)$$

$$B=-\frac{1}{2}\left[\frac{\Theta_0}{R_0}+\left(\frac{d\Theta}{dR}\right)_0\right], \quad (5)$$

where the velocities and derivatives at R_0 are calculated from the polynomial fit (3). The results for H II regions, Type I, Type I + IIa and Type I + II PN are also given in Table 7. According to recent work, the value of A is broadly in the range 12–17 km s^{-1} kpc^{-1}, and for B the range is (-9)–(-15) km s^{-1} kpc^{-1} (cf. Mihalas & Binney 1981, chapter 8; Rohlfs et al. 1986). The average uncertainties are 10–15% (constant A) and about 20% (constant B). It can be seen that the results shown in Table 7 are in good agreement with these values, within the uncertainties. The same is true for the circular velocity at the Sun's position, which is only slightly less than the adopted value, considering an uncertainty of the order of 10% (Knapp 1983).

Acknowledgements. WJM thanks A. Zijlstra for some private communication, and C.C.M. Leite for some discussions. This work was partially supported by CNPq.

References

Acker A., 1978, A&AS 33, 367
Acker A., 1980, A&A 89, 33
Amnuel P.R., Guseinov O.H., Novruzova H.I., Rustamov Yu.S., 1984, ApSS 107, 19
Barker T., Cudworth K.M., 1984, ApJ 278, 610
Blitz L., 1979, ApJ 231, L115
Blitz L., Fich M., Stark A.A., 1980, in: Andrew B.H. (ed.) IAU Symposium 87. Reidel, Dordrecht, p. 213
Blitz L., Fich M., Stark A.A., 1982, ApJS 49, 183
Blitz L., 1983, in: Shuter W.L.H. (ed.) Kinematics, dynamics and structure of the Milky Way. Reidel, Dordrecht, p. 143
Burton W.B., Gordon M.A., 1978, A&A 63, 7
Chini R., Wink J.E., 1984, A&A 139, L5
Clemens D.P., 1985, ApJ 295, 422
Daub C.T., 1982, ApJ 260, 612
Dutra C.M., Maciel W.J., 1990, Rev. Mex. Astron. Astrofis. 21, 264
Faúndez-Abans M., Maciel W.J., 1986, A&A 158, 228
Faúndez-Abans M., Maciel W.J., 1987, A&A 183, 324
de Freitas Pacheco J.A., Veliz J.G., 1987, MNRAS 227, 773
Gathier R., Pottasch S.R., Goss W.M., 1986b, A&A 157, 191
Gathier R., Pottasch S.R., Pel J.W., 1986a, A&A 157, 171
Knapp G.R., 1983, in: Shuter W.L.H. (ed.) Kinematics, dynamics and structure of the Milky Way. Reidel, Dordrecht, p. 233
Maciel W.J., 1984, A&AS 55, 253
Maciel W.J., 1987, in: Kwok S., Pottasch S.R. (eds.) Late Stages of Stellar Evolution. Reidel, Dordrecht, p. 391
Maciel W.J., 1989, in: Torres-Peimbert S. (ed.) IAU Symposium 131. Kluwer, Dordrecht, p. 73
Maciel W.J., 1992, in: Terlevich R.J. (ed.) Elements and the Cosmos. Cambridge University Press, Cambridge (in press)
Maciel W.J., Faúndez-Abans M., 1985, A&A 149, 365
Maciel W.J., Leite C.C.M., 1992, in: Barbuy B. (ed.) IAU Symposium 149. Kluwer, Dordrecht (in press)
Maciel W.J., Faúndez-Abans M., Oliveira M., 1986, Rev. Mex. Astron. Astrofis. 12, 233
Méndez R.H., Kudritzki R.P., Herrero A., 1992, A&A (in press)
Mihalas D., Binney J., 1981, Galactic Astronomy, 2nd. ed., Freeman, San Francisco
Peimbert M., 1978, in: Terzian Y. (ed.) IAU Symposium 76. Reidel, Dordrecht, p. 215
Peimbert M., 1990, Rep. Prog. Phys. 53, 1559
Peimbert M., Torres-Peimbert S., 1983, in: Flower D.R. (ed.) IAU Symposium 103. Reidel, Dordrecht, p. 233
Peña M., Ruiz M.T., Maza J., González L.F., 1989, Rev. Mex. Astron. Astrofis. 17, 25
Peña M., Ruiz M.T., Torres-Peimbert S., Maza J., 1990, A&A 237, 454
Peralta J.O., 1978, A&A 64, 127
Reid M.J., 1989, in: Morris M. (ed.) IAU Symposium 136. Kluwer, Dordrecht, p. 37
Rohlfs K., Chini R., Wink J.E., Böhme R., 1986, A&A 158, 181
Sabbadin F., 1986, A&AS 64, 579
Schneider S.E., Terzian Y., 1983, ApJ 274, L61
Schneider S.E., Terzian Y., Purgathofer A., Perinotto M., 1983, ApJS 52, 399
Shuter W.L.H., 1982, MNRAS 199, 109
Torres-Peimbert S., Peimbert M., Peña M., 1990, A&A 233, 540
Zijlstra A.A., Pottasch S.R., 1991, A&A 243, 478